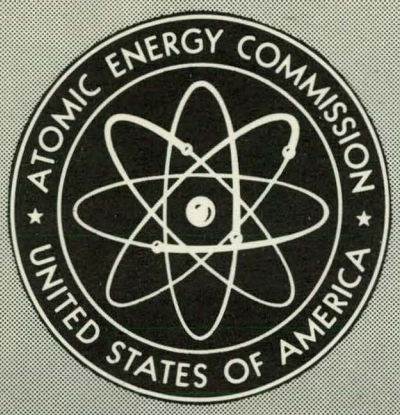

GEAP-3997

EXAMINATION OF 304 STAINLESS STEEL CLADDING FROM COLD-SWAGED AND ROLLED FUEL RODS

By
W. V. Cummings
D. R. Lewis
R. E. Blood

July 1962

Vallecitos Atomic Laboratory
General Electric Company
San Jose, California

UNITED STATES ATOMIC ENERGY COMMISSION • DIVISION OF TECHNICAL INFORMATION

DISCLAIMER

LEGAL NOTICE

Printed in USA. Price $1.00. Available from the Office of Technical Services, Department of Commerce, Washington 25, D. C.

USAEC Division of Technical Information Extension, Oak Ridge, Tennessee

PAGES i to ii

WERE INTENTIONALLY

LEFT BLANK

GEAP-3997

METALS, CERAMICS,
AND MATERIALS

EXAMINATION OF 304 STAINLESS STEEL CLADDING FROM COLD-SWAGED AND ROLLED FUEL RODS

By

W. V. Cummings

D. R. Lewis

R. E. Blood

July 1962

U.S. Atomic Energy Commission
Contract AT(04-3)-361

VALLECITOS ATOMIC LABORATORY

GENERAL ELECTRIC

ATOMIC POWER EQUIPMENT DEPARTMENT
SAN JOSE, CALIFORNIA

TABLE OF CONTENTS

LIST OF ILLUSTRATIONS

LIST OF TABLES

1.0 INTRODUCTION

The characteristics of a fuel element cladding material can be changed substantially by the fabricating process associated with the manufacture of the fuel element. This is particularly true in the case of compacted powder type fuel fabricated by swaging or rolling. These fabricating processes introduce from twenty-five to thirty per cent cold work into the cladding. Samples of cladding from unirradiated fuel rods fabricated by cold swaging and tandem rolling[1][2] were submitted for investigation to determine the effects of cold working on the properties of 304 stainless steel. The cladding samples were representative of fuel rods fabricated for irradiation testing under High Power Density Development Project.

The methods used for the study were tensile testing, metallography, and X-ray diffraction. The results of tensile tests reveal the strength and ductility of the metal and the nature of the fractures both before and after cold working. Metallographic examination discloses the effect of swaging and rolling over the fuel on the inside surface of the cladding, reveals the presence of second phases or precipitates, and in general, characterizes the microstructure. Any crystallographic preferred orientation that is developed in the cladding during the swaging and rolling procedures can be indicated by the nature of the microstructure, but can be determined quantitatively only by X-ray diffraction. The determination of preferred orientation is important in order to relate the anisotropic effects that can be predicted from these measurements to mechanical properties and microstructure, and from this correlation predict the behavior of the cladding under various operating conditions.

2.0 SUMMARY

The properties of 304 stainless steel cladding for uranium dioxide fuel have been examined in the as-received condition and following cold swaging and tandem rolling. Metallographic examination of the cladding showed an expected cold work texture, as well as some limited amount of UO_2 penetration of the clad ID. The maximum penetration was limited to about 20 per cent of the wall thickness. Mechanical tests at both room temperature and 650°F show that these cold working operations increase the yield and ultimate strengths. The mechanical properties in the cold worked cladding at 650°F also are greater than in the as-received material at room temperature. However, the nature of the 650°F fractures in the cold worked cladding is drastically modified from those in the cold worked material tested at room temperature, and also from those breaks in the as-received material tested at both temperatures. Preferred orientation measurements disclose that this fracture angle coincides with the position of a maximum population of (111) planes.

It is proposed that the differences in the fracture behavior that is observed is the result of a strain-induced transformation of the face-centered structure of austenite to the body-centered structure of ferrite or martensite in the immediate vicinity of the break.

From these studies, metallurgical and mechanical properties of stainless steel cladding from unirradiated swaged and rolled fuel rods have been defined. The results indicate that the studied clad properties should be adequate for boiling water nuclear fuel. The effect of neutron irradiation on these properties would be difficult to deduce from available literature data.

3.0 DETAILS OF EXPERIMENTAL INVESTIGATION

3.1 Clad Specimen Preparation

The fuel rod cladding used in the investigation was obtained from fabricated fuel rods identical in all respects to fuel rods fabricated for irradiation testing.[3] The fuel rods were fabricated by cold swaging[1] and tandem rolling.[2] Starting clad size (as-received) was 0.500 inch OD x 0.015 inch wall. Finished size of the clad after swaging or rolling was 0.400 inch OD x 0.015 inch wall. The UO_2 was removed from the fuel rod by dissolution using nitric acid. A typical chemical analysis of the as-received 304 stainless steel cladding is presented in Table I.

3.2 Mechanical Testing

3.2.1 Testing Procedure

Mechanical tests were performed on two representative samples of cold swaged and tandem rolled cladding, and also on the original cladding in the as-received condition. Tensile coupons were taken from a four inch region just off the center of the clad. Six transverse (circumferential) coupons were cut from each of the clad types and three longitudinal coupons were cut from the cold swaged clad. The coupons were obtained by slitting the clad on one side and then laying it out flat so as to form sheet material. A small amount of cold work ($\sim$2%) was unavoidably introduced during this procedure.

Sheet tensile specimens were then machined from these coupons with a guage length of 0.250 inch for the transverse specimens and 0.634 inch for the longitudinal specimens. Figure 1 shows the dimensions of the machined test specimens. Three transverse tensile tests were performed for each of the clad types at room temperature and at 650°F. For the cold swaged longitudinal

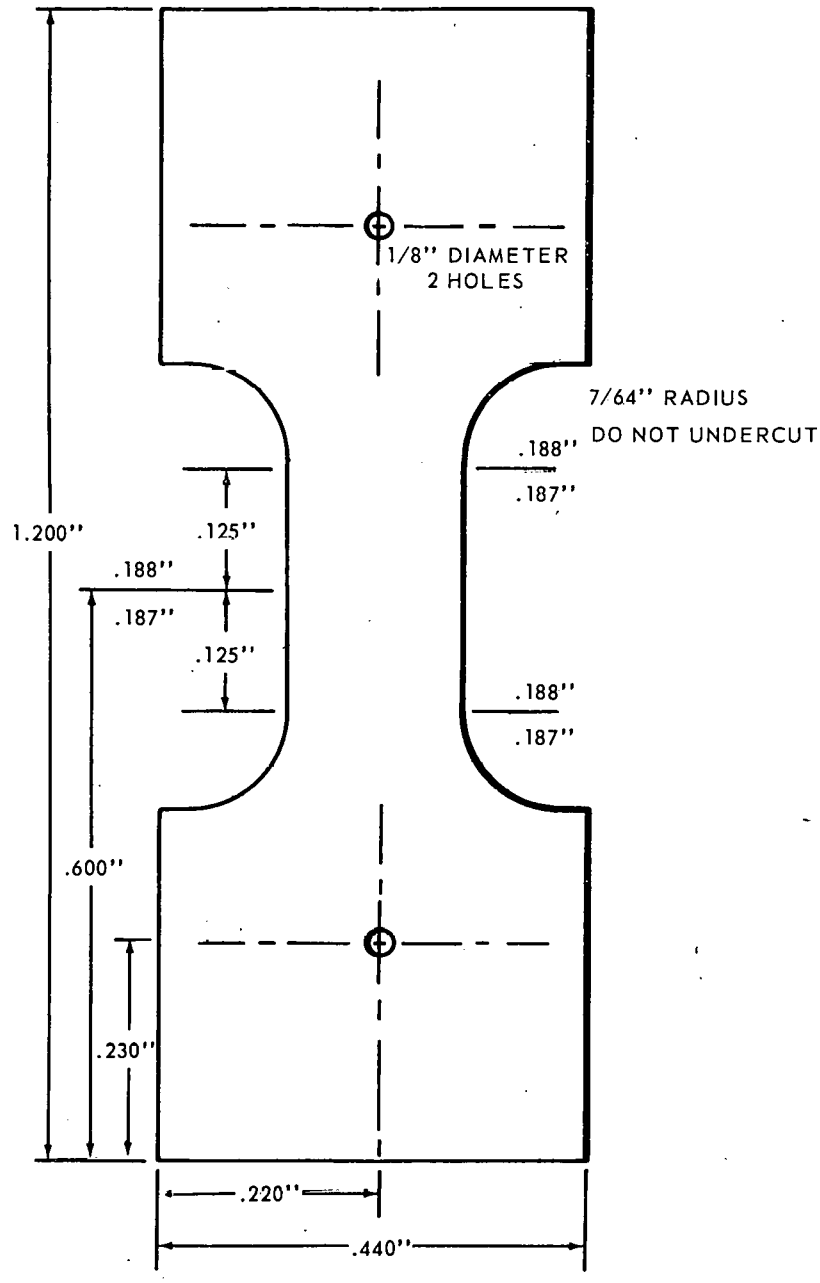

760-8

FIGURE 1 SHEET TENSILE SPECIMEN

TABLE I.

CHEMICAL ANALYSIS OF AS-RECEIVED 304 STAINLESS STEEL CLADDING

C	Mn	P	S
.023	1.47	.008	.015
Si	Ni	Cr	Co
.58	10.93	18.50	.06

specimens, one was tested at room temperature and two were tested at 650°F. Testing was done on a standard 12,000 pound universal testing machine. Values were taken from a stress-strain recorder attached to the machine.

3.2.2 Test Results

Average values for all tests performed are tabulated in Table II. Yield strengths were obtained from a 0.2% offset. Uniform elongation for the as-received specimens was not obtained but closely approaches the total elongation value because of the almost complete absence of localized necking.

From Table II it can be seen that, in general, the yield and ultimate strengths were greatly increased by both the cold swaged and tandem rolled processes, but with the cold swaged values somewhat lower than the tandem rolled values. Also, the yield strengths were increased with respect to the ultimate strengths for both cold swaged and rolled processes. The observed increase in tensile strength is expected due to the cold work (36% RA) introduced by rolling and swaging.

In the as-received transverse tubing tested at room temperature, high elongation with practically no localized necking was observed. The specimens fractured in a generally ragged manner but displayed some tendency to break at angles ranging from 25° to 45° to the longitudinal direction of the tubing. The specimens tested at 650°F showed high elongation although less than those tested at room temperature and localized necking also was low. Of the three as-received specimens tested at 650°F, two broke near the shoulder, one with a ragged fracture and the other with a somewhat angular break, but the third

TABLE II

TENSILE DATA FOR SWAGED AND ROLLED 304 STAINLESS STEEL CLADDING

Specimen	Yield Strength 0.2% Offset (kpsi)		Ultimate Strength (kpsi)		Total Elongation (%)		Reduction of Area (%)		Uniform Elongation (%)	
	R.T.	650 F	R.T.	650 F	R.T.	650 F	R.T.	650 F	R.T.	650 F
As-received transverse	55.9	39.1	103.7	73.9	76.0	37.2	53.2	32.8	--	--
Cold swaged transverse	94.1	82.3	125.4	102.4	31.5	10.0	45.2	46.9	7.0	3.2
Tandem rolled transverse	112.1	100.8	141.0	116.1	20.8	8.0	31.9	42.6	4.7	2.5
Cold swaged longitudinal	108.9	88.6	131.7	107.1	19.9	4.1	40.5	45.4	11.6	2.1

broke in the center of the gauge length at an angle of about 60° to the tube axis. Figure 2 illustrates the nature of specimen fracture.

Elongation in the cold swaged transverse specimens at room temperature was much less than that of the as-received material. The fracture was uneven with rather localized necking. There was no indication of an angular type fracture. Elongation in the cold swaged specimens tested at 650°F was drastically reduced from the as-received values. Necking was extremely localized and was confined to an area within 0.02 inch on either side of the fracture. All three specimens fractured with the smooth 30° angular fracture which was common to all the 650°F tests, except for some of the as-received samples. The basic difference between these breaks and those of the 650°F as-received specimens was the extremely localized nature of the fracture.

Elongation in the tandem rolled transverse specimens tested at room temperature also was greatly reduced from the as-received specimens and also somewhat lower than the cold swaged values. Localized necking seem to be about the same as in the cold swaged specimens although reduction of the area was slightly lower. The fracture was very similar to that of the cold swaged specimens. Elongation in tandem rolled specimens tested at 650°F also was drastically lower than that in the as-received material and slightly lower than in the cold swaged. Like the 650°F swaged specimens, necking was extremely localized and confined to the area within 0.02 inch on either side of the fracture. The fracture was the same shape, cleavage-like fracture displayed by the cold swaged specimens. Reduction of area was

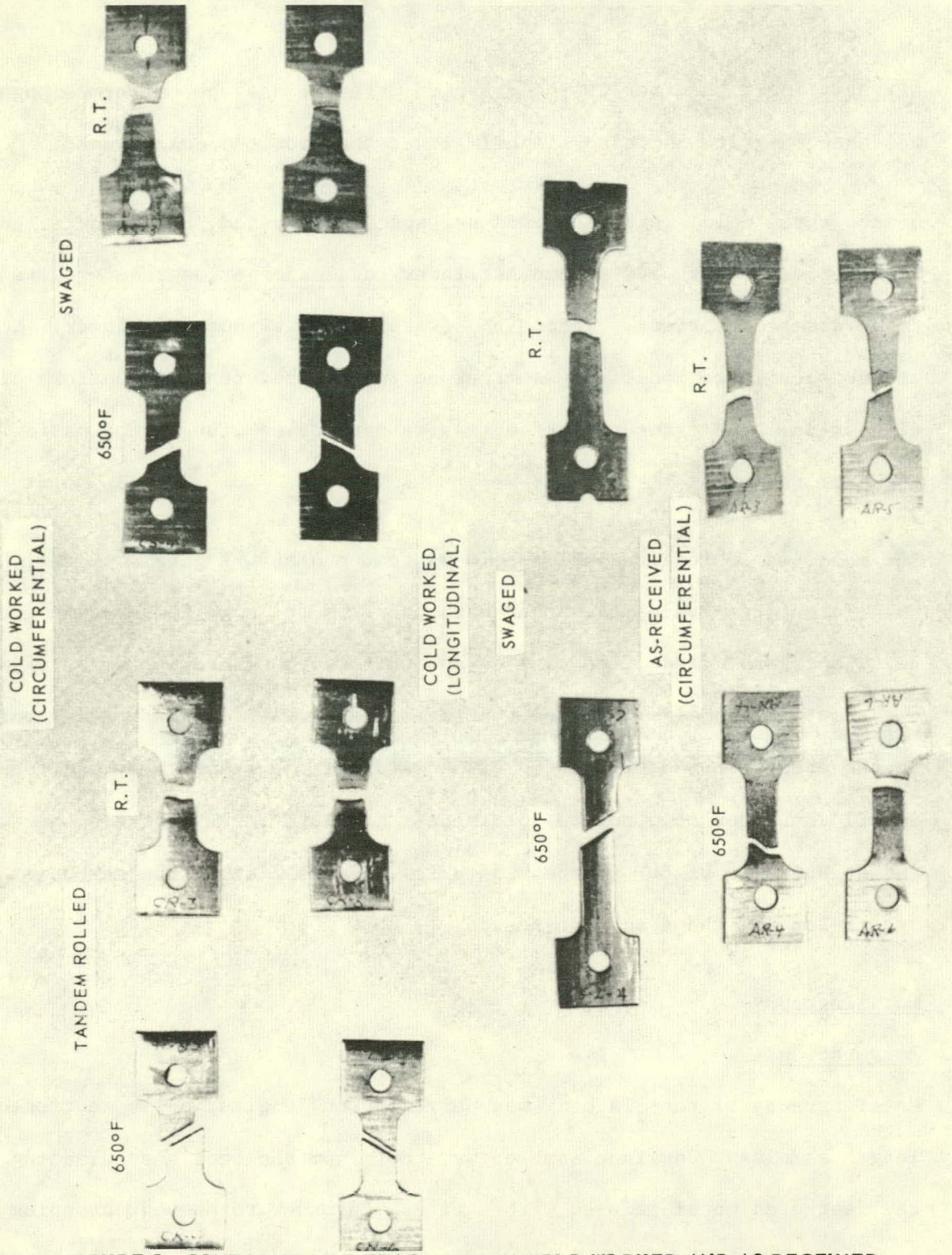

FIGURE 2 COMPARISON OF FRACTURES IN COLD WORKED AND AS-RECEIVED 304 STAINLESS STEEL CLADDING TESTED AT ROOM TEMPERATURE AND 650°F.

760–7

slightly lower than for the cold swaged material and the uniform elongation was extremely low and also slightly lower than for the cold swaged.

Of the three cold swaged longitudinal specimens tested, the ones tested at room temperature showed a somewhat lower total elongation than did its transverse counterpart. Reduction of area also was somewhat lower. Necking was not nearly as localized as might be interpreted from the uniform elongation value. The fracture surface was rather uneven with no indication of an angular fracture.

The cold swaged longitudinal specimens tested at 650°F gave a slightly lower total elongation value than that obtained from the high temperature transverse specimen. Reduction of area and uniform elongation were approximately the same. Extremely localized necking was apparent and was mostly confined to the area within 0.02 inch on either side of the fracture as was found in all the other cold worked specimens. Similarly, the fracture was sharp and at an angle of 60° to the tube axis. Figure 2 shows the nature of the breaks for all the specimens tested.

3.3 Metallography

3.3.1 Preparation

Metallography of the cladding was performed on longitudinally sectioned full length samples. One inch samples were cut from the sectioned cladding and the feathered metal removed with a file. In order to prevent crushing of the samples during mounting it was necessary to add a small amount of bakelite to the mold before the sample was inserted. This bakelite acted as a cushion

and prevented the tube from springing when the pressure was applied during the mounting procedure. The excess bakelite was removed with a belt sander.

The samples were ground through 600 grit silicon carbide abrasive paper and rough polished with six micron diamond. Final polishing was done with a vibratory polisher with one micron diamond on microcloth. Kerosene was used as a lubricant. The final polishing time varied but was seldom longer than eight hours.

All specimens were electrolytically etched with 10% oxalic acid. Because of the configuration of the samples and the different wall thickness, it was difficult to determine the exact current density used. Experimentally, however, it was found that four volts for approximately one minute gave a satisfactory etch. Electrical contact with the specimen was made by a stainless steel screw tapped through the back of the mount.

Cladding from five separate fuel rods were prepared for full longitudinal examination. They were identified as follows:

TABLE III

Fabrication Process	Fuel	Use
Cold swaged	Natural fused UO_2 powder	Prototype
Cold swaged	Enriched fused UO_2 powder	Assembly 2S
Tandem rolled	Natural fused UO_2 powder	Prototype
Tandem rolled	Enriched fused UO_2 powder	Assembly 3S
Swaged over pellets	Natural UO_2 pellets	Prototype

In addition to the cladding, an as-received tube was examined.

3.3.2 Examination

As-Received Tubing (Figure 3)

The microstructure of the as-received tubing appeared normal. ASTM grain size was measured to be No. 6. Considerable oxide slag inclusion was observed throughout the cladding.

Cold Swaged - Prototype (Figure 4)

The microstructure of this tube was typical of cold worked 304 stainless steel. The grains were highly distorted and often elongated in the direction of working. Slip lines were visible in all of the samples. In addition to the usual slip lines, "flow lines" or lines of deformation could be seen throughout the tube wall in the direction of swaging. These lines formed a wavy pattern which appeared to flow the full length of each specimen but showed a slight misalignment at the grain boundaries.

Both the inside and outside surfaces of the tube wall were so severely cold worked that the detail of the structure was difficult to resolve.

Almost all of the samples showed numerous oxide stringers of a second phase which ran longitudinally through the tube. The stringers observed in the as-received tubing generally were short. Some stringers had aligned with others to give total lengths of approximately five mils. A few of the stringers measured as much as 12 mils. Some deformation was noted along the inside surface of the tube but these irregularities were in the form of shallow and rounded depressions. No sharp or deep indentations were observed.

150 X

FIGURE 3 AS RECEIVED TUBING, LONGITUDINAL SECTION

760–4

150 X

FIGURE 4 COLD SWAGED, PROTOTYPE, LONGITUDINAL SECTION

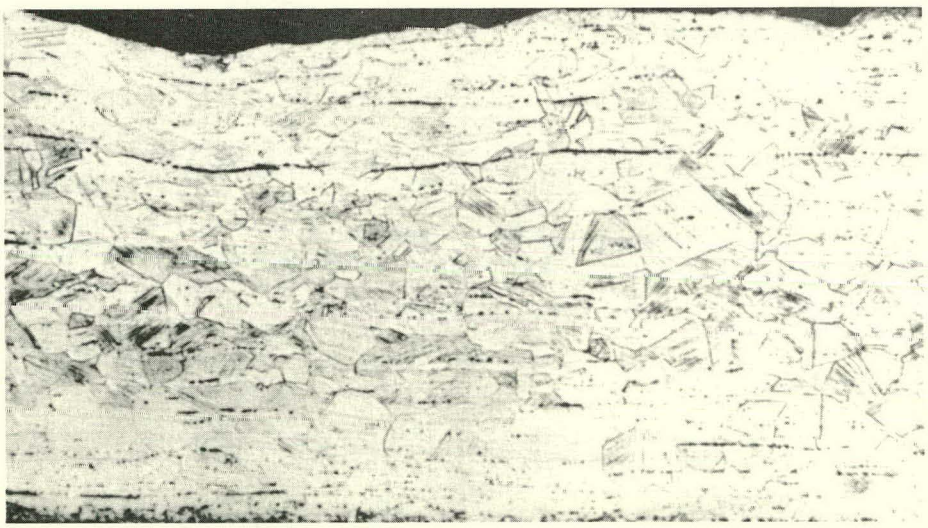

150 X

FIGURE 5 COLD SWAGED, ASSEMBLY 2S, LONGITUDINAL SECTION

760–5

Cold Swaged - Assembly 2S (Figure 5)

The microstructure of this tube was similar to that of the prototype cladding. Slightly less stringering of the second phase was observed although individual samples showed severe stringering for short distances.

Damage to the inside diameter of the tube was slightly more severe than that of the prototype in spite of the fact that the fabrication process of both tubes was the same. This difference could be just normal variation between rods.

Carbide precipitation in the grain boundaries of the end plug and in the tube adjacent to the plug was noted. The precipitate formed a continuous network from the OD to the ID of the cladding. This type of pattern is susceptible to intergranular corrosion.[4]

Tandem Rolled - Prototype (Figure 6)

The microstructure and appearance of the inside diameter of this tube is very similar to that of the prototype cold swaged tube. With only a few exceptions, deformation of the tube wall was minor and damage was in the form of shallow depressions rather than sharp indentations.

Sensitization of the tube adjacent to the end plug again was visible. Carbide precipitation appeared to be more extensive and severe than the sensitized zone in the cold swaged tube.

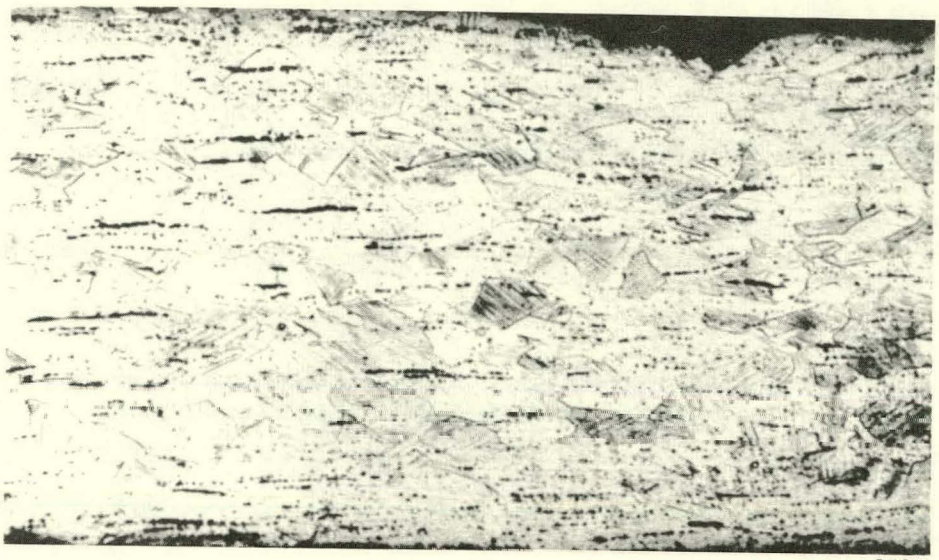

150X

FIGURE 6 TANDEM ROLLED, PROTOTYPE, LONGITUDINAL SECTION

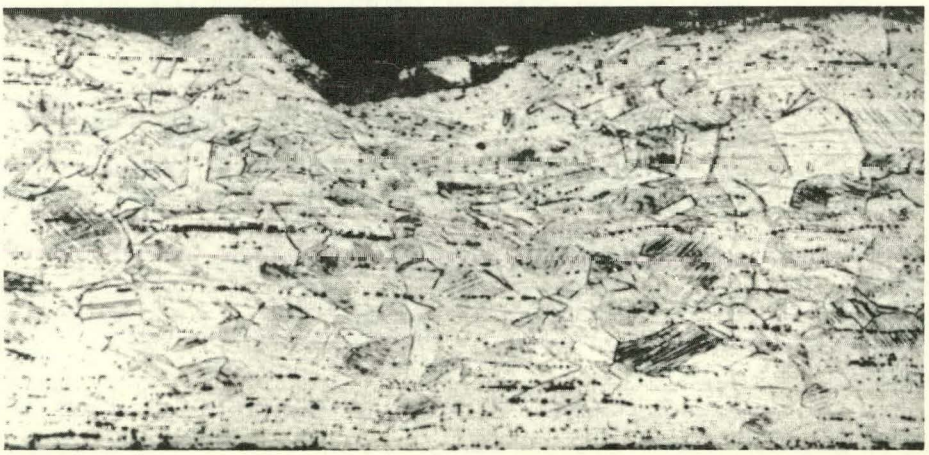

150 X

FIGURE 7 TANDEM ROLLED, ASSEMBLY 3S, LONGITUDINAL SECTION

760–6

Tandem Rolled - Assembly 3S (Figures 7 and 8)

This tube was spot checked and not examined completely as were the others. Six longitudinal and six transverse specimens were taken and prepared for microscopic examination.

Although fabrication of this element was identical with that of the tandem rolled prototype described above, several angular indentations of the clad were observed. The longitudinal specimens were by far the most severely distorted of any of the other tubes. Examination of the transverse samples revealed even deeper indentations. Maximum clad penetration observed was four mils into the tube wall.

The increase in damage to the tube wall in the 2S and 3S assemblies as compared to the respective prototype tubes indicates a possible difference in the swaging characteristics of the enriched UO_2 used in these rods. However, since only one rod of the prototype and one of the actual assembly rods was examined, there is the possibility that inadequate sampling is the cause of the observed variations.

Swaged Over Pellets (Figure 9)

Six tubes of this type were examined metallographically. Macro examination of the inside of the tube revealed "markings" made by the contact of each pellet. These areas appeared to be depressions made by the compaction of the clad around the pellet. The tubes were sampled in such a way that each mount contained at least one complete pellet mark.

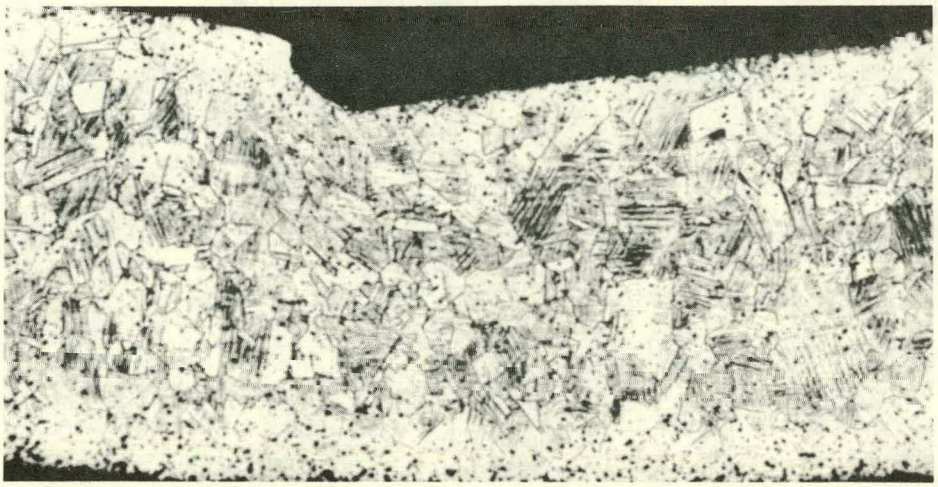

150X

FIGURE 8 TAMDEN ROLLED, ASSEMBLY 3S, CROSS SECTION

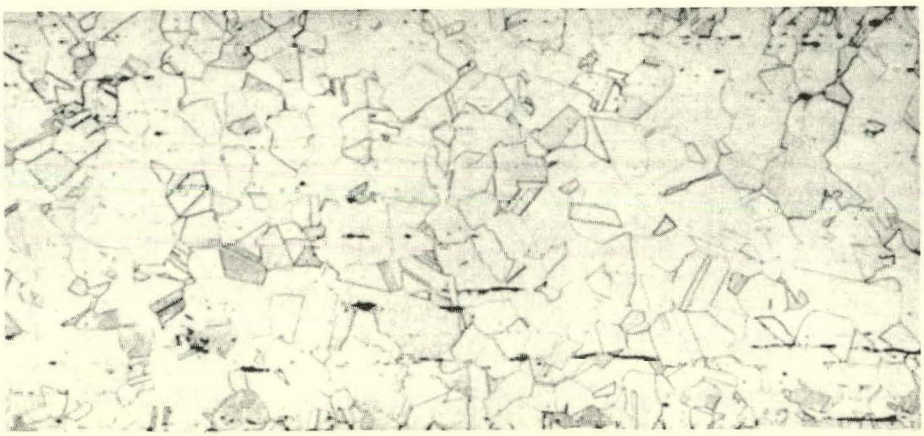

150X

FIGURE 9 SWAGED OVER PELLET, PROTOTYPE

760–3

The microstructure of the tube wall was that of lightly worked 304 stainless steel. Slip lines could be seen in many of the grains, but distortion and elongation of the grains was slight.

Both the inside and outside surfaces of the tube were very uniform. There was no evidence that the "markings" observed during the macroscopic examination were actually depressions which penetrated or indented the tube wall.

Distortion of the inside surface of the tube was found in only one area. This was in the form of flowed metal and appeared to be the result of movement of a fuel pellet during swaging. This area of flowed metal disappeared after regrinding two mils below the examined surface.

Photomicrographs of typical distorted area of each of the five tubes examined are shown in Figures 4 - 9.

Tensile Specimens

Metallographic examination was performed on the as-received, cold swaged, and tandem rolled specimens after they were tensile tested. Both room temperature and elevated temperature tested samples were prepared and examined in an effort to determine the reason for the types of fractures encountered.

At first it was thought there might be a relationship between the fracture angle and the stringers of second phase, but it was found that no such relationship existed. The fractures ran parallel, perpendicular, and at 45 degree angles to the stringers, but no consistent pattern was found nor was any effect of stringer orientation observed.

On the basis of magnetic tests and X-ray diffraction analysis which suggested the presence of a body centered cubic phase (ferrite or martensite) the samples were reprepared and etched to reveal the martensite, if present. The etchant used consisted of 25 grams of CrO_3, 133_2 cc acetic acid, and 7 cc water at 0.2 amps/inch for three minutes. Because of the extreme thinness of the samples, the electrolytic etch produced a severely rounded edge at the fracture even though edge preservation was excellent after the final polish. The rounding effect seriously hampered the taking of photomicrographs although visual examination was not obstructed.

Cold work in the immediate vicinity of the fracture was so severe that details of the structure were not clearly resolved. This obliteration of structural detail is similar to that observed on the outside surface of the swaged and rolled tubing.

Examination of the specimens at high magnification (1000X) showed that martensite was present. At lower magnifications the martensite was not easily discernable because of its similarity in appearance to slip lines.

Martensite plates were observed in all the samples examined, with the exception of the as-received tubing tested at 650°F. However, considerably less of this phase was observed in the 650°F samples as shown in Figures 10 and 11. Variation in the amount of martensite present was observed from area to area of each sample.

The as-received tubing tested at 650°F contained no martensite (Figure 12) while the specimen pulled at room temperature (Figure 13) contained

1000X

FIGURE 10 COLD SWAGED TENSILE SPECIMEN TESTED AT 650°F

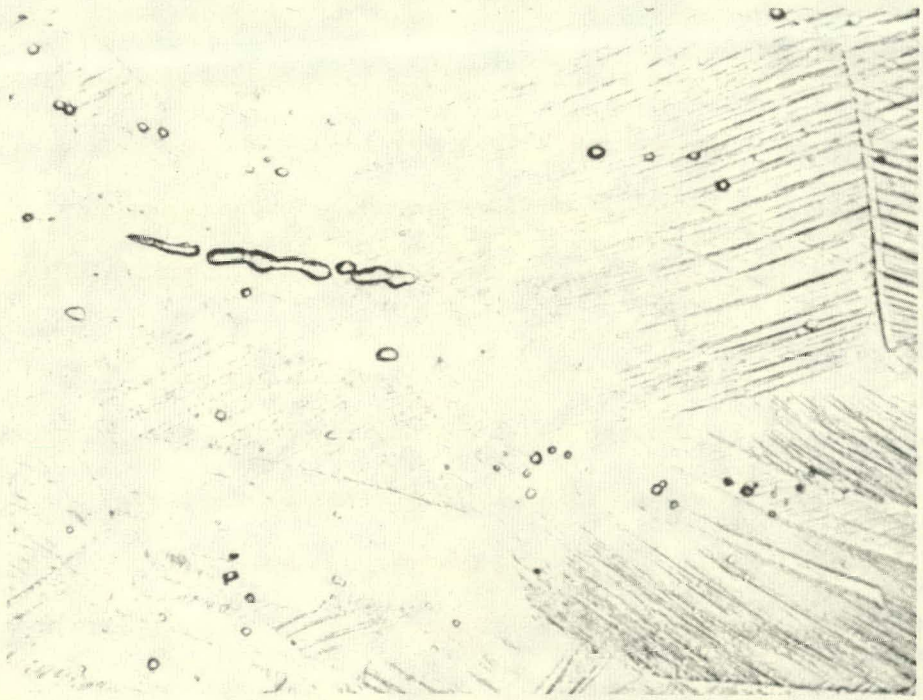

1000 X

FIGURE 11 TANDEM ROLLED TENSILE SPECIMEN TESTED AT ROOM TEMPERATURE

760–2

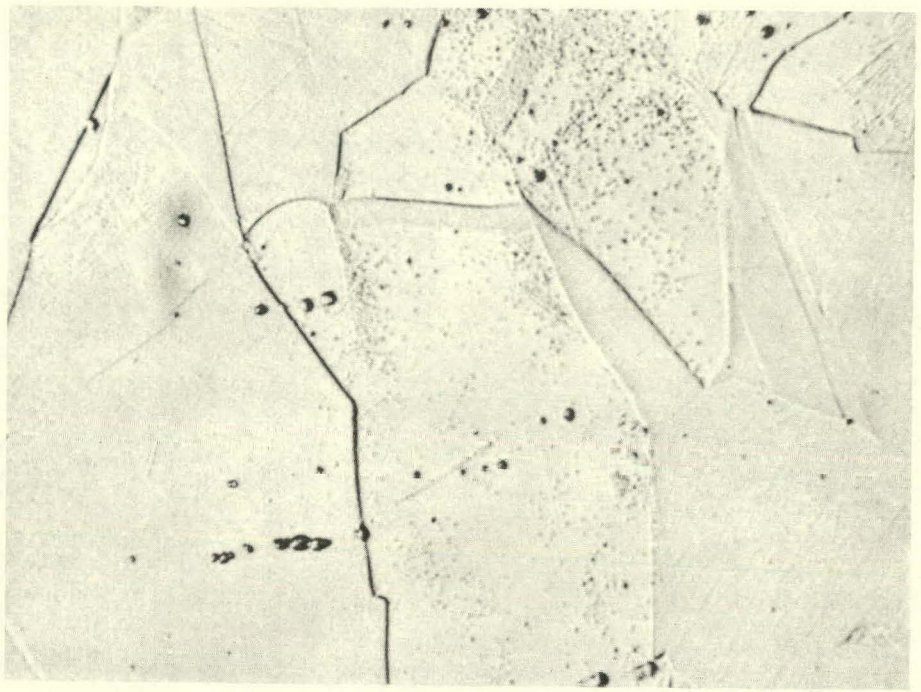

1000 X OBLIQUE LIGHT

FIGURE 12 AS RECEIVED TUBING TENSILE SPECIMEN TESTED AT 650°F

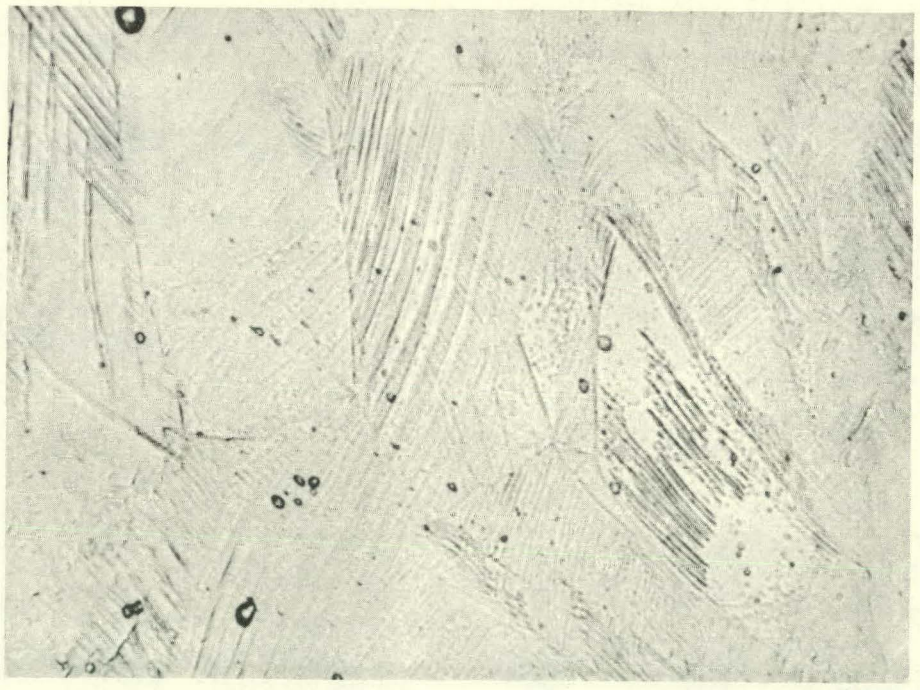

1000 X

FIGURE 13 AS RECEIVED TUBING TENSILE SPECIMEN TESTED AT ROOM TEMPERATURE

760-1

slightly less than that observed in the room temperature tested rolled coupon.

Although X-ray diffraction analysis showed the largest amount of martensite at the fracture, the obliteration of detail caused by the amount of cold work prevented identification of any significant increase in this material near the fracture edge.

3.4 Preferred Orientation

3.4.1 Method

The mechanical working or deformation of metals almost invariably produces a preferential alignment of the grains about some crystallographic direction. The type and magnitude of the preferred orientation that is developed is dependent upon the deformation systems within the crystal and the nature of the applied forces. Since the mechanical and physical properties of crystals are in general anisotropic, it is important to determine the crystallographic preferred orientation of the grains that is developed in 304 stainless fuel cladding during rolling and swaging operations. X-ray diffraction is used to determine the three dimensional distribution of a number of (hkl) crystallographic poles and this distribution is plotted on a stereographic net in the form of a pole figure.

This work was performed with the use of a spiral scanning goniometer mounted on the diffractometer of a General Electric XRD-5 X-ray unit. The spiral scanning technique is basically the Schulz method as modified by Holden.[5] The specimen is simultaneously rotated through two angles ϕ and α whose

axes are always mutually perpendicular. The axis of rotation for ϕ is horizontal and its position is defined by the plane that includes the face of the sample, the plane defined by the incident and diffracted X-ray beams, and the main axes of the diffractometer. The maximum angular scan for ϕ is 90°. The axis of rotation for α intersects the rotational axis for ϕ and is always perpendicular to the sample face. The ratio of angular speeds for the two motions is 1°-ϕ to 60°-α. This ratio provides intensity data from a particular (hkl) reflection along a spiral path that has a 6° pitch. These angular motions are driven synchronously with the strip chart recorder so that the intensity data may be read directly and plotted on the stereographic projection with minimum difficulty.

Experimental Procedures

Intensity data that is sufficient for a complete pole figure is impossible to obtain from one sample. As the tilt angle ϕ increases, both defocusing and absorption of the X-ray beam affects the intensity of the diffracted X-rays. Some steps can be taken to minimize these effects, but the practical limit for the ϕ rotation is about 60°. To circumvent this problem, three mutually perpendicular sample faces are used, each of which is tilted less than the 60° limit. The intensity data from the three spiral scans can then be projected to correct positions on a stereographic net as shown in Figure 14 for a full description of the preferred orientation.

For the tubular cladding in this study, the three directions are radial (parallel to a radius), transverse or tangential (tangent to the circumference), and longitudinal (parallel to the tube axis). Specimens for the

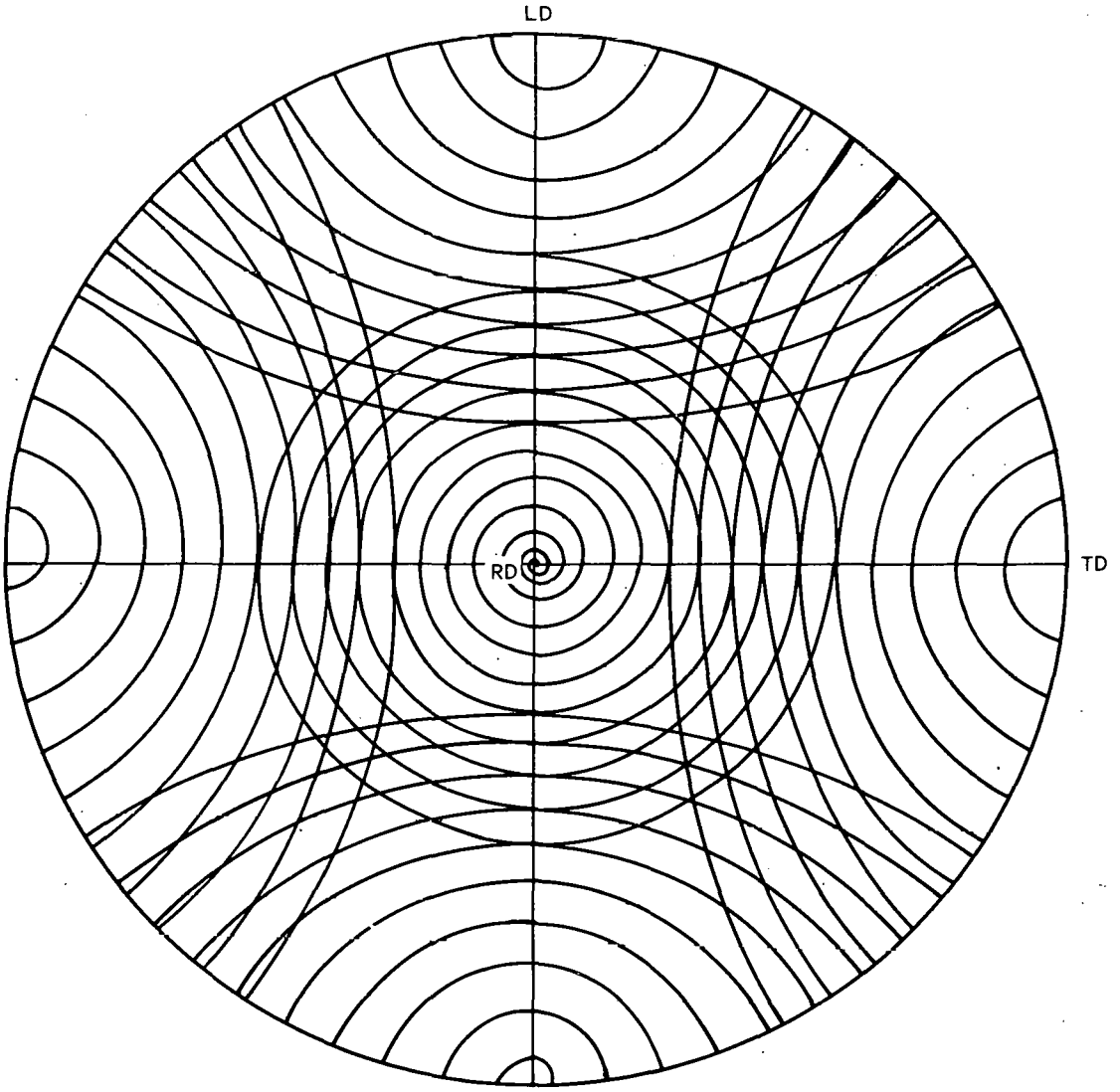

FIGURE 14 SUPERIMPOSED SPIRALS ON A STEREOGRAPHIC NET FOR PLOTTING CORRECTED INTENSITY READINGS

760–9

radial shots were easily obtained since a single section cut from the tubing provides a large area for the sample face. To obtain the specimen area for the longitudinal and transverse shots, however, it was necessary to cut several sections from the thin walled tubing and to stack these sections so that areas of approximately one square centimeter were obtained. After clamping the sections firmly in the correct orientation with respect to the tube axis, the two perpendicular faces representing longitudinal and transverse directions were prepared for X-ray diffraction by grinding and electropolishing. This method of specimen preparation was used for all three types of cladding.

The most descriptive and quantitative method of presenting the magnitude of preferred orientation is to convert the intensity data to multiples of the intensity obtained from a random sample. This ratio method of description also has the added advantage of not requiring a correction for absorption and defocusing. To provide a standard with complete random orientation, a sample was prepared by hydrostatically pressing 304 stainless steel powder into a compact. Three perpendicular faces were then prepared from which intensity data was obtained along the three spiral paths described above. No significant variation in the angular intensity distribution from the three faces was observed. This sample was used as a random standard in this study. A correction was made in the random intensity to compensate for the lower than theoretical density of the powder compact.

Results

Complete pole figures for the (111), (200) and (220) planes were obtained for the as-received, tandem rolled and cold swaged cladding. These plots are shown in Figures 15 through 23. Only one quarter of the figure is shown since symmetry is apparent in tube material. An experimental check also showed this assumption to be true. The pole figures obtained from the (200) and (220) reflections are designated by their first order nomenclature (100) and (110).

It can be seen in Figures 15, 16 and 17 that steep gradients or intensity contours that deviate appreciably from the random value of 1.0 do not exist in the pole figures representing the as-received tubing. The largest amount of orientation in this material is found in the (110) pole figure. A poorly defined maxima with values from 1.6 to 1.4 times random ranges through the 90° area between the radial and transverse directions. This means that a greater than random number of (110) planes lie parallel to the axis of the tube and are distributed about this line in a varying, but always greater than random density. The (111) and (100) pole figures show that these planes are even more randomly oriented in the as-received material. The maxima are ill-defined and have values of only 1.2 times random.

A large amount of preferred orientation is produced in the cladding by both the tandem rolling and swaging action. In addition, the orientations produced by the two methods of cold working are qualitatively the same. The maxima do differ by a few degrees and the orientation values for these maxima are in general slightly higher in the swaged material.

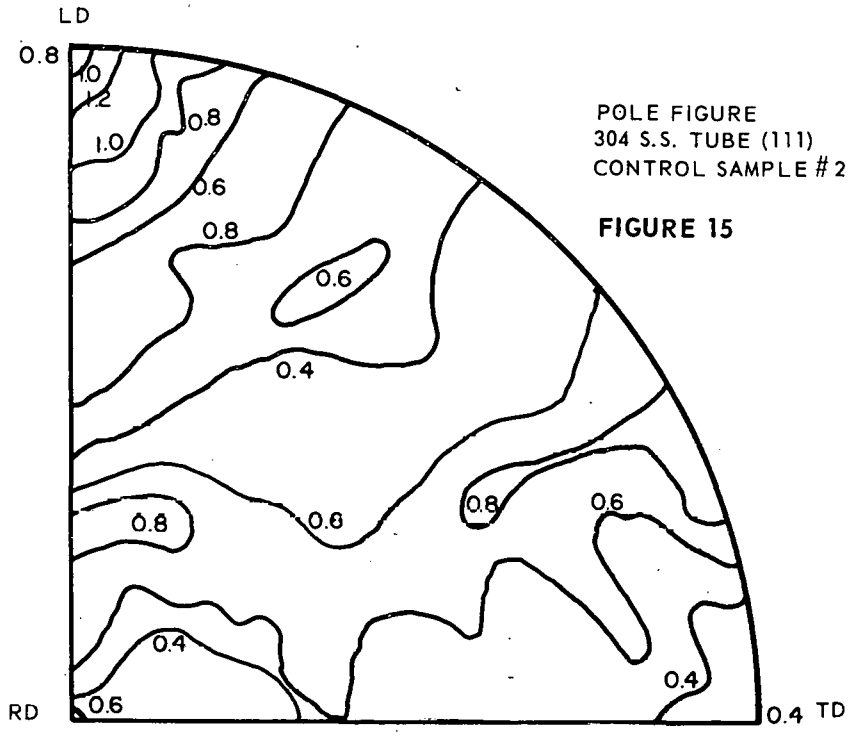

POLE FIGURE
304 S.S. TUBE (111)
CONTROL SAMPLE # 2 (AS RECEIVED)

FIGURE 15

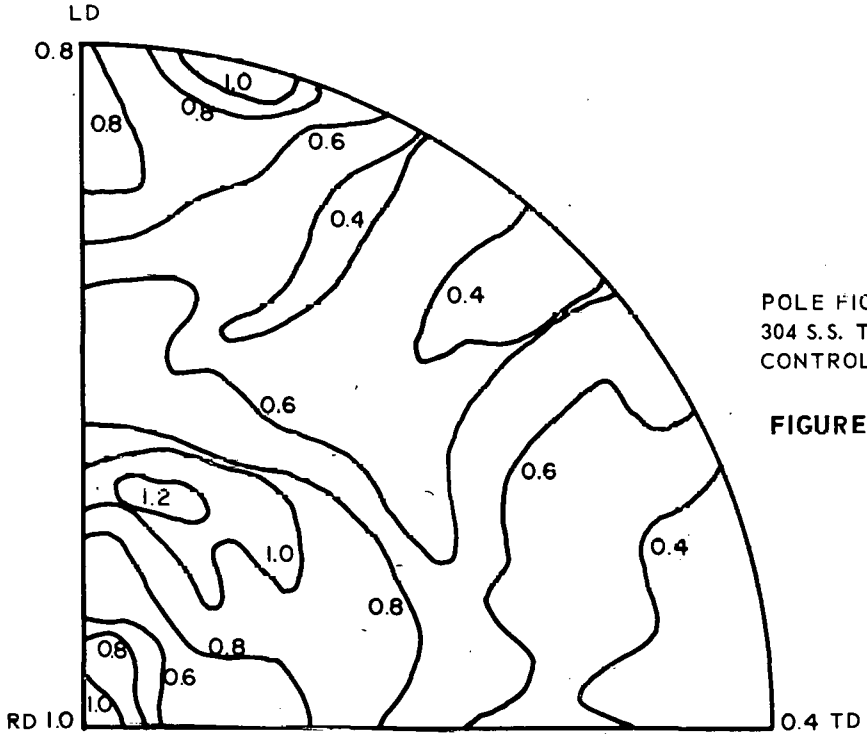

POLE FIGURE
304 S.S. TUBE (200)
CONTROL SAMPLE # 2

FIGURE 16

760–11

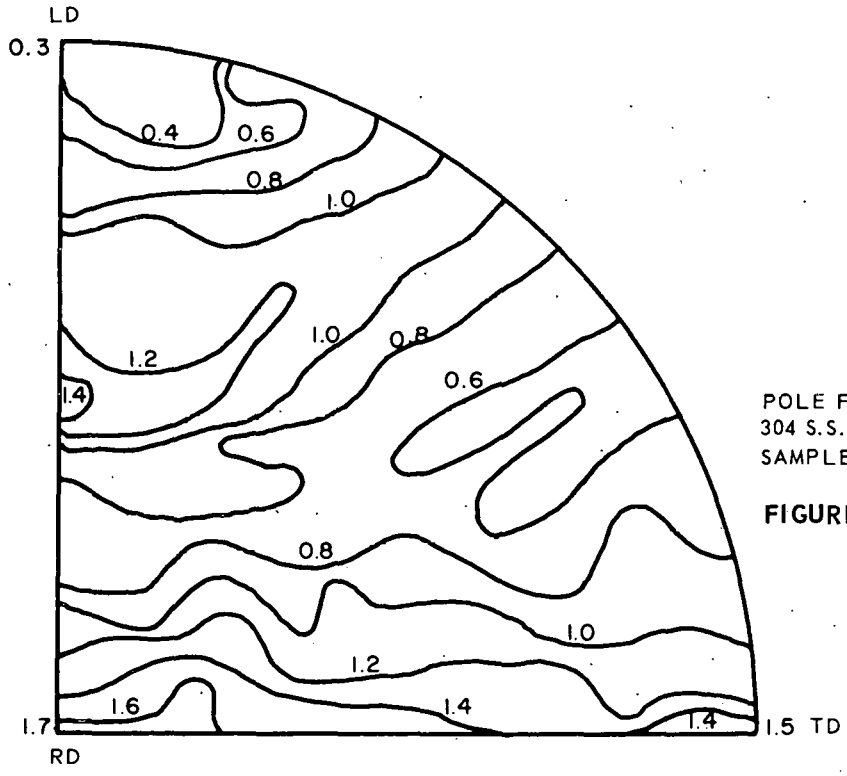

POLE FIGURE
304 S.S. TUBE (220)
SAMPLE # 2 CONTROL

FIGURE 17

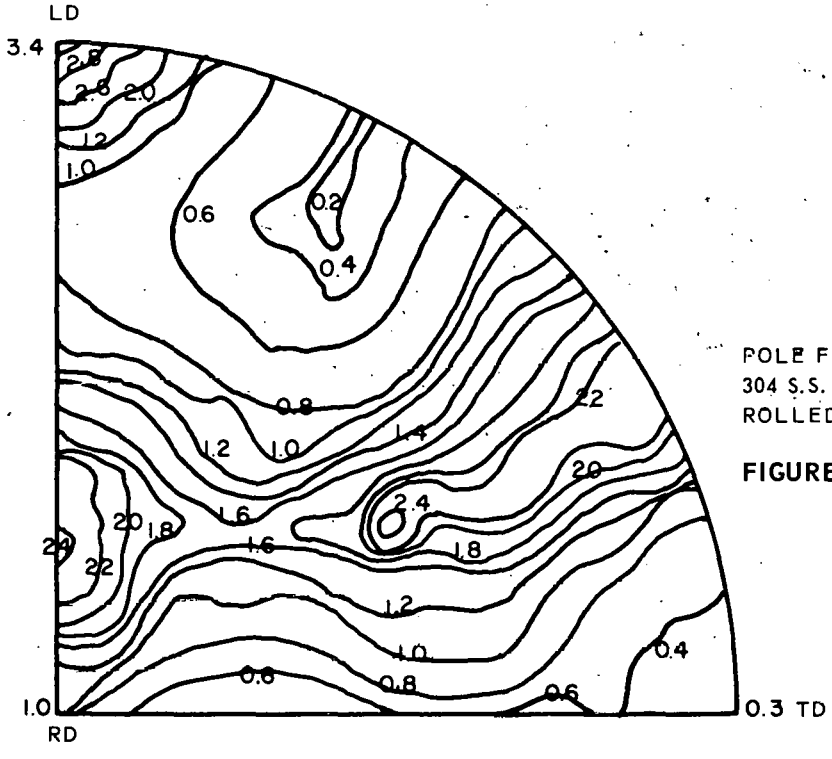

POLE FIGURE
304 S.S. TUBE (111)
ROLLED SAMPLE # 1

FIGURE 18

760–10

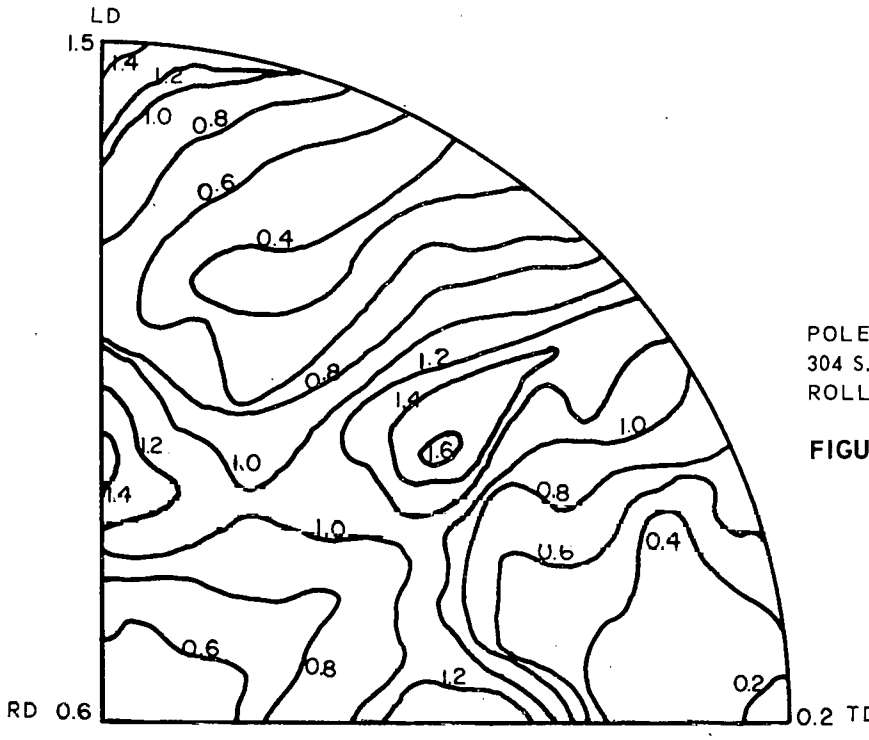

POLE FIGURE
304 S.S. TUBE (200)
ROLLED SAMPLE # 1

FIGURE 19

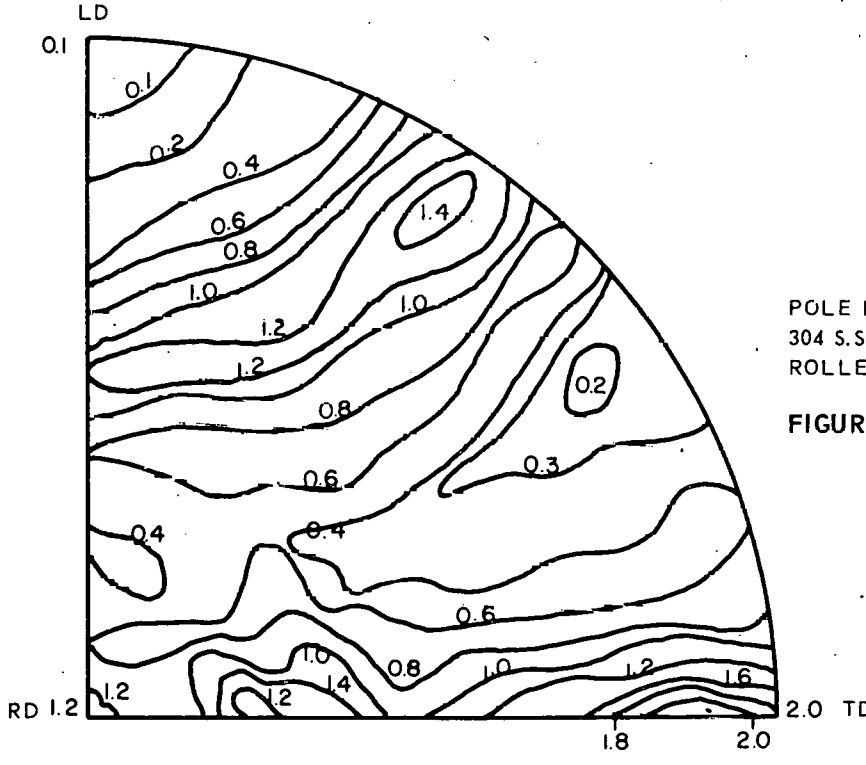

POLE FIGURE
304 S.S. TUBE (220)
ROLLED SAMPLE # 1

FIGURE 20

760–12

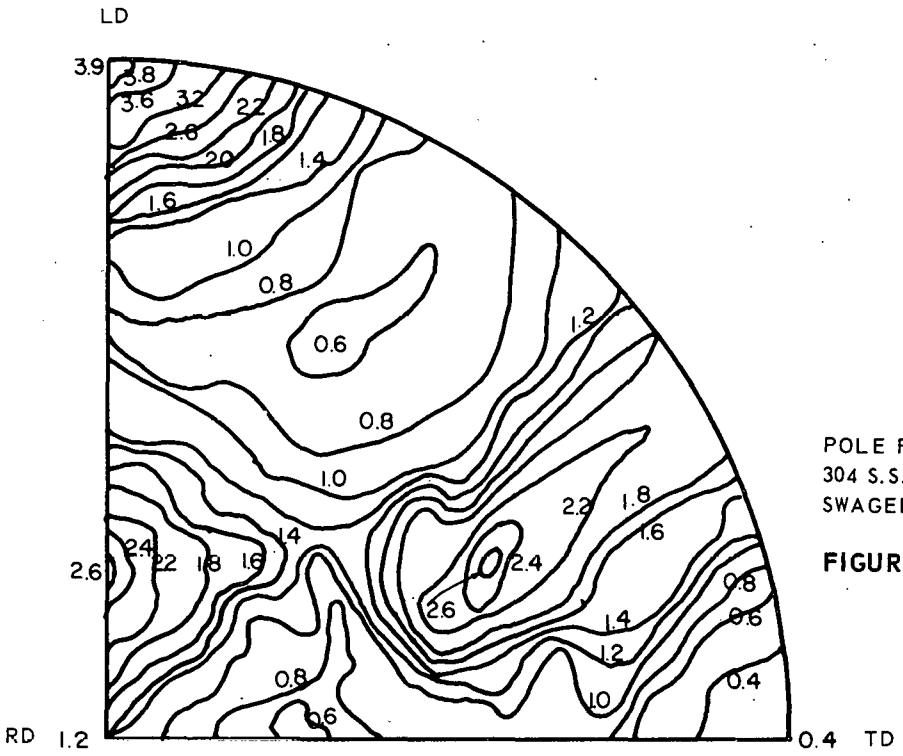

POLE FIGURE
304 S.S. TUBE (111)
SWAGED SAMPLE # 3

FIGURE 21

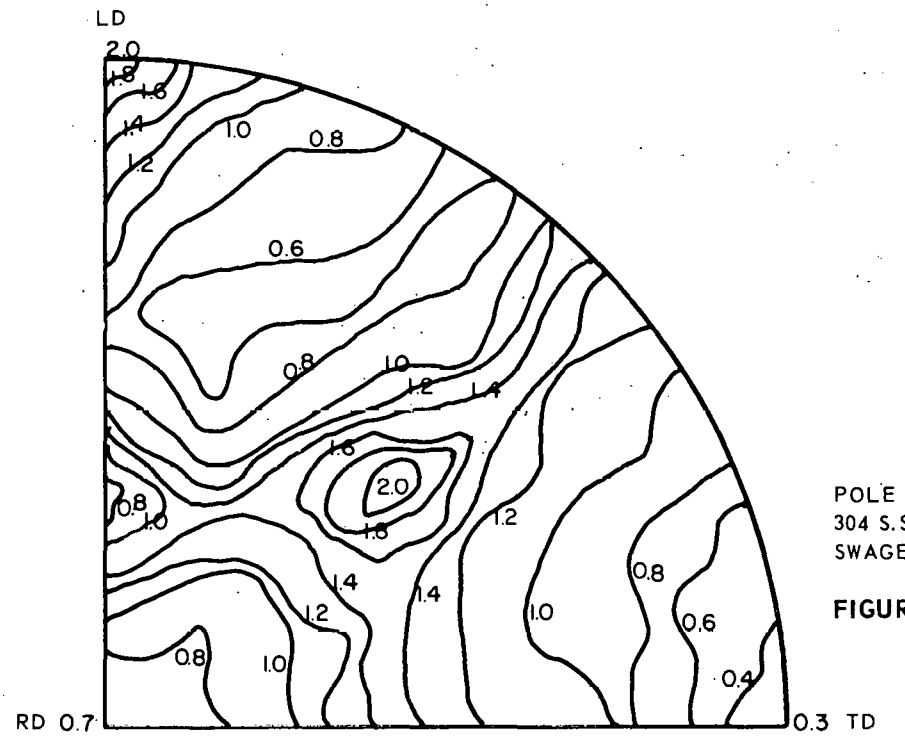

POLE FIGURE
304 S.S. TUBE (200)
SWAGED SAMPLE # 3

FIGURE 22

760-13

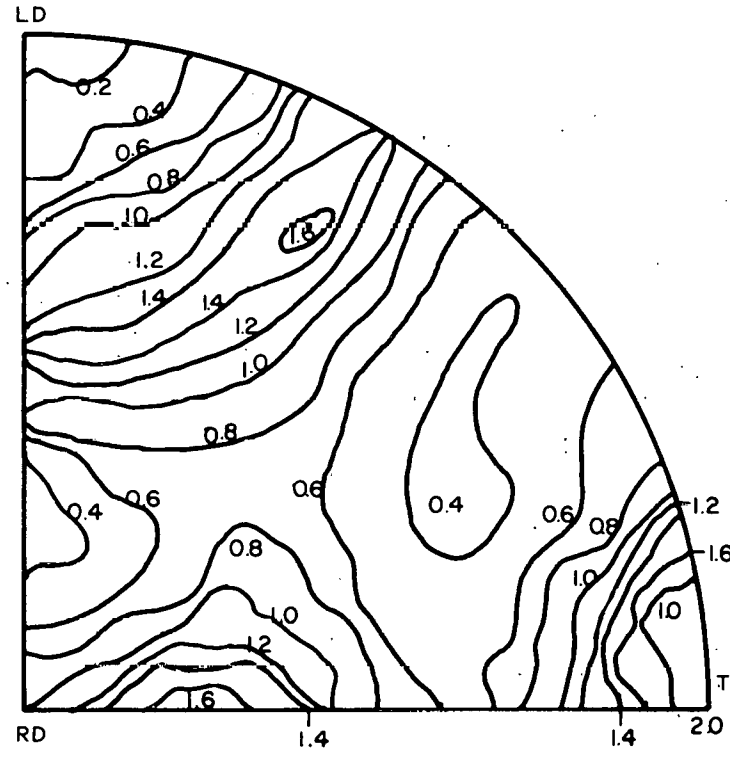

POLE FIGURE
304 S.S. TUBE (220)
SWAGED SAMPLE #3

FIGURE 23

760-14

In both cold worked materials, a maximum density of (111) planes lie perpendicular to the tube axis. Remembering that $\emptyset$ is the angular tilt from the radial direction and α is the rotation about this radial direction with 0° defined as the tube axis, this (111) maximum position is described as $\emptyset = 90^{\circ}$, $\alpha = 0^{\circ}$. The magnitude of the orientation at this point is 3.4 and 3.9 times random for the rolled and swaged materials, respectively. Other (111) maxima of lesser magnitude are found at $\emptyset = 30^{\circ}$, $\alpha = 0^{\circ}$ and $\emptyset = 60^{\circ}$, $\alpha = 60^{\circ}$.

The (100) pole figures for the two cold worked materials show maxima at approximately $\emptyset = 90^{\circ}$, $\alpha = 0^{\circ}$ and $\emptyset = 60^{\circ}$, $\alpha = 50^{\circ}$. A maximum of lesser magnitude also is indicated at $\emptyset = 40^{\circ}$, $\alpha = 0^{\circ}$. The orientation values for these points are less than those for the (111) high density positions by an approximate factor of one-half.

The (110) maxima are at angular positions of $\emptyset = 90^{\circ}$, $\alpha = 90^{\circ}$; $\emptyset = 30^{\circ}$, $\alpha = 90^{\circ}$; and $\emptyset = 80^{\circ}$, $\alpha = 30^{\circ}$.

All of the values for angular positions shown above are rounded to the nearest 5°. The best measured values of both angular position and orientation magnitude at these positions are given in Table IV.

TABLE IV.

PREFERRED ORIENTATION DATA AND BREAK ANGLES

Specimen Ident.	Pole Fig. (hkl)	Max. Dens. Poles (hkl) Ø	Max. Dens. Poles ∝	Orientation Value (X Random)	Break Angle** Room Temp.	Break Angle** 650°F	Remarks
As-received	(111)	nearly random			not clearly defined range 30°-45°	fairly well defined at either 60° or 90°	ductility decreased at 650°F
	(100)	nearly random					
	(110)	52°	0°	1.4			
		(90°	90°	1.4			
		*(0°	90°	1.6			
Tandem rolled	(111)	90°	0°	3.4	not clearly defined ~90°	58°	ductility drastically decreased; sharp angular breaks at 650°F
		30°	0°	2.4		58°	
		60°	60°	2.4		58°	
	(100)	90°	0°	1.5			
		42°	0°	1.4			
		66°	51°	1.6			
	(110)	84°	32°	1.4			
		81°	90°	2.0			
		26°	90°	1.4			
Cold swaged	(111)	90°	0°	3.9	not clearly defined ~90°	62°	ductility drastically decreased; sharp angular breaks at 650°F
		31°	0°	2.6		64°	
		66°	63°	2.8		64°	
	(100)	90°	0°	2.0			
		37°	0°	1.8			
		58°	50°	2.0		58°	
						64°	
	(110)	79°	30°	1.6			
		90°	90°	2.0			
		28°	90°	1.6			

*Continuous range between these angular positions

**Angular relation to pole figure

4.0 DISCUSSION

The nature of the fractures at room temperature in the as-received tubing is normal and is what would be expected from annealed and randomly oriented 304 stainless steel. The slip plane in face-centered cubic materials (austenitic stainless steel) is the (111) plane. These materials usually behave in a ductile manner and when randomly oriented break at 45° because this is the direction of the maximum resolved shear stress. The alloying elements no doubt modify the tensile behavior to a certain extent, but the effect would not be expected to be large. It is also known that at low temperatures strain will cause the formation of body-centered cubic ferrite in the metastable austenite.[6] This transformation is quite active below room temperature, and is still pronounced at room temperature for large strains. Body-centered cubic metals behave quite differently from those with face-centered cubic structures as far as tensile properties are concerned and can in general be expected to fracture in a brittle manner. It was noted from magnetic tests on the broken specimens that a considerable amount of ferrite had been formed in the immediate vicinity of the fracture.

The fracture of the annealed, as-received material when tested at 650°F seems to have occurred rather abruptly following a ductile deformation similar to the initial behavior of the room temperature specimens. The fracture occurred, however, before an equal elongation had been reached. Examination of the surfaces show that the fractures were partially at 60° and partially at 90° to the direction of the applied tensile force, Figure 2. In some cases, both angles of fracture were apparent in the same specimen. Microscopic examination of the thin section of the broken specimen disclosed that

in general the portion of the specimen that broke at 60° to the direction of the applied force fractured at approximately 90° to the surface of the tube. In addition, the portion that broke at 90° to the force direction fractured at approximately 45° in the thin dimension. Magnetic tests showed that very little ferrite was formed in the vicinity of the high temperature breaks.

In order to obtain more quantitative data on the austenite to ferrite transformation, pinhole back reflection X-ray photographs were obtained from both the fracture surfaces and the undeformed portions of the tensile specimens. By using chromium X-radiation and a specimen to film distance of 4.0 cm, the austenite (220) and ferrite (211) reflections were recorded simultaneously. Only ferrite was detected at the fracture surfaces of the specimens pulled at room temperature. Conversely, only austenite was detected at the fracture surfaces of the specimens pulled at 650°F. Since the slight amount of magnetism caused by the cold swaging and rolling persists after heating to 650°F, undoubtedly a small amount of ferrite is present in these samples but in concentrations below the limit of detectibility. This limit also applies to small amounts of austenite in ferrite in the room temperature samples. This lower limit can be expected to be less than five per cent. The undeformed sections of all the test specimens remained austenitic and again, even though the cold worked specimens were slightly magnetic in these areas, the amount of ferrite formed by cold swaging and rolling was insufficient for detection by X-ray diffraction.

The results of these measurements definitely show that at room temperature the material in the immediate vicinity of the fracture has transformed

almost completely from austenite to ferrite but at 650°F essentially no transformation occurs.

The room temperature tensile properties of both the swaged and tandem rolled specimens are typical of cold worked metals. The only difference in the properties of the two is in the magnitude of the cold worked effect. The measured effects are an increase in yield and ultimate strengths and a decrease in total elongation and reduction in area as compared to the as-received state. Table II shows that these changes were slightly larger in the tandem rolled specimens. As would be expected, a small amount of ferrite was formed during the cold working making the material slightly magnetic. After breaking, the specimens were very ferritic in the immediate vicinity of the fracture. The breaks were ragged but generally at 90° to the direction of the tensile force in the major surface of the specimen but at approximately 45° to the direction perpendicular to this surface.

The tensile properties of the two types of cold worked material are markedly changed by raising the temperature to 650°F. Although the yield and ultimate strengths decrease a small amount, these properties are still well above those for the as-received material tested at room temperature. However, the total elongation has dropped to only a few per cent and the deformation has all occurred within 0.02 inches of the break. The angle of fracture is very uniform and well defined and can be measured precisely in the major surface of the specimen. In the rolled specimens this angle is 58° to the direction of the applied tensile force. For the cold swaged specimen, this angle is 62° - 64° for the transverse specimens and 58° - 64° to this same direction

for the longitudinal specimens. These data along with data from the pole figures showing the positions of maximum pole density for the various planes are shown in Table IV. Figure 2 also shows the nature of the fractures as described above.

Further observation of the fractures in the cold worked, high temperature specimens disclose that no additional ferrite is formed at the break as a result of the testing.

The tensile properties of the cold worked 304 stainless at 650°F are unusual and evidently behavior of this type has not been reported previously. This temperature is below that necessary for carbide formation and well below that necessary for instability of the austenite to be a factor. No correlation is found with the direction of the stringers that were observed metallographically. One relationship that is apparent, however, is the direction of preferred orientation of the (111) planes to the angle of fracture. What is actually represented by the angle of fracture in the plane of the tube surface is the angular component in the stereographic plane defined by the longitudinal and transverse directions in the pole figure. This fracture angle in every high temperature specimen of cold worked material can be related to a (111) maxima in the corresponding pole figure. A maximum number of (111) poles occur at an angle of 60° in this resolved plane for the rolled cladding and the measured angle of break is 58°, or within 2°, of being parallel to the (111) planes. In the cold swaged tubing these angles are 63° for the maxima in the pole figure and range from 58° to 64° for the break. Two other (111) maxima exist in the pole figures but the (111) planes in both cases are parallel to the applied tensile force and the resolved shear stresses are zero.

The angle of fracture to the direction perpendicular to the tube surface is difficult to determine in the thin walled tubing. A microscopic examination, however, revealed that the breaks in the cold worked tubing tested at 650°F occurred in every case in the range of 60 to 90 degrees to the tube surface. The (111) maxima are at 60 and 66 degrees in the tandem rolled and swaged tubing, respectively. However, an examination of the equidensity contours in both (111) pole figures, Figures 18 and 21, shows that the population of (111) planes is quite high over the entire range from the maximum positions indicated to a full 90° to the tube surface. For instance, in the rolled sample, the orientation value is 2.4 times random at 60° or the position of the maxima and is still greater than 2.2 times random at 90°. In the swaged sample these values are 2.6 and 2.0, respectively. The fractures can, therefore, be related directly to a region that has a high density of (111) planes parallel to the fracture surface.

The angle of fracture in the cold worked tubing tested at 650°F can be correlated to the measured preferred orientation of the (111) planes. On the other hand, the room temperature fractures in the same cold worked material cannot be related to the pole figures as derived for the face-centered cubic system. A large amount of ferrite (or martensite) was formed in the immediate vicinity of the fracture in the room temperature specimens but not in the high temperature specimens. This observation strongly suggests that the room temperature break actually occurs in a small volume of highly strained material that is primarily body-centered ferrite rather than face-centered austenite. Since the measured preferred orientation is for the face-centered cubic structure, it cannot be related to the room temperature

ferritic fractures except by coherency relationships. In any event, fractures in body-centered cubic materials are inherently of a discontinuous and serrated nature such as is observed in the cold worked room temperature test specimens. The strain-induced transformation of austenite to ferrite is temperature dependent and for large strains a substantial amount of ferrite is produced at room temperature. This transformation, however, decreases rapidly with increasing temperature and should be completely inactive at 650°F. The fractures at this temperature, therefore, should be characteristic of face-centered cubic structures and should be related to the measured preferred orientation.

The direction of the high temperature fractures in the cold worked cladding are definitely related to the preferred orientation, but the yield and ultimate strengths are much greater than would be expected for ductile face-centered cubic materials. In addition, the strain to fracture is very low. This behavior is evidently a result of the retention at 650°F of the major portion of the high strength properties that are produced by cold working and of the rapid propagation of the fracture along the oriented (111) planes once yielding is initiated.

5.0 CONCLUSIONS

The metallurgical and mechanical properties of stainless steel cladding from unirradiated swaged and rolled fuel rods have been defined to a considerable degree. The effect of swaging and rolling on the clad grain structure was found to be that of producing a structure containing a large amount of slip bands. The swaging and rolling also caused limited UO_2 particle penetration into the clad ID. The extent of particle penetration observed was 0.004 inch, maximum.

The tensile strength properties of the swaged and rolled cladding were increased over the starting properties of the tubing, whereas the ductility was decreased. Yield strength at 650°F was 39,000, 82,000 and 101,000 psi for starting tubing, swaged clad and rolled clad, respectively. Elongation at 650°F was 37%, 10% and 8%, respectively.

The fracture behavior of the swaged and rolled clad was different from the starting tubing. Preferred orientation measurements and metallographic examination of the fractures showed this difference to be due to a preferential orientation of the (111) planes in the cold worked cladding.

The results of this work indicate that the properties of swaged and rolled cladding that were studied should be adequate for fuel rods irradiated in a boiling water reactor. The effect of neutron irradiation and boiling water coolant environment on the cladding properties was not determined in this investigation.

REFERENCES

1. GEAP-3918, "Fuel Element Fabrication by Swaging," E. A. Lees, April, 1962.

2. GEAP-3775, "Fabrication of Fuel Rods by Tandem Rolling," J. W. Lingafelter, July, 1961.

3. GEAP-3717, "Fourth Quarterly Progress Report, Jan-March, 1961."

4. Stickler, R., and Vinckier, A., "Morphology of Grain Boundary Carbides and Its Influence on Intergranular Corrosion of 304 Stainless Steel," Trans. ASM, Vol. 54, 1961.

5. Holden, A. N., "A Spiral-Scanning X-Ray Reflection Goniometer for the Rapid Determination of Preferred Orientations," Rev. Sci. Instr., Vol. 24, No. 1, p. 10, 1953.

6. Fiedler, H. C., Averbach, B. L., Cohen, M., "The Effect of Deformation on the Martensite Transformation in Austenite Stainless Steel," Trans. ASM, Vol. 47, 1955.